



Dielectric functions and energy band gap variation studies of manganese doped $\text{Bi}_{3.25}\text{La}_{0.75}\text{Ti}_3\text{O}_{12}$ thin films using spectroscopic ellipsometry



Priekshit Gautam^{a,b,*}, Anupama Sachdeva^a, Sushil K. Singh^c, R.P. Tandon^a

^a Department of Physics and Astrophysics, University of Delhi (DU), Delhi 110007, India

^b Department of Physics Kirori Mal College, University of Delhi, Delhi 110007, India

^c Functional Materials Division, SSPL, Timarpur, New Delhi 110054, India

ARTICLE INFO

Article history:

Received 1 July 2014

Received in revised form 28 July 2014

Accepted 30 July 2014

Available online 7 August 2014

Keywords:

Ferroelectric thin films

Chemical solution deposition

Optical properties

Spectroscopic ellipsometry

ABSTRACT

Single phase polycrystalline Mn-modified $\text{Bi}_{3.25}\text{La}_{0.75}\text{Ti}_3\text{O}_{12}$ (BLT) thin films were prepared by chemical solution deposition method using spin coating technique on Pt/Ti/SiO₂/Si (100) substrates. Raman spectroscopy of these films shows that Mn³⁺ is well substituted at Ti⁴⁺ site. The optical properties of BLT and Mn modified BLT thin films were investigated at room temperature by using spectroscopic ellipsometry (SE) in the energy range 0.72–6.2 eV. A double Tauc–Lorentz (DTL) dispersion relation was successfully used to model the dielectric functions of these films where a shift to the lower energy side with Mn doping is seen. The full width at half maxima (FWHM) (Γ) of dielectric function is found to increase with Mn doping. This increase in FWHM may be attributed to the increase in the trap density in forbidden band which consequently decreases the value of direct optical band gap (E_g^d). The direct optical band gap (E_g^d) is found to decrease with increase in Mn content in the studied composition range. This decrease in E_g^d with doping may be attributed to the variation in the defect concentration present in the structure.

© 2014 Elsevier B.V. All rights reserved.

1. Introduction

Thin films of bismuth-based layer structured ferroelectric (BLSF) compounds such as $\text{SrBi}_2\text{Ta}_2\text{O}_9$ (SBT), $\text{Bi}_4\text{Ti}_3\text{O}_{12}$ (BT) and related materials are of interest for variety of integrated device applications, such as optical memory and electro-optic devices [1–4]. SBT ($n = 2$) and BT ($n = 3$) belong to the class of aurivillius phases with layered intergrowth structures which consist of ‘ n ’ layers of perovskite-like blocks sandwiched between two consecutive fluorite-like (Bi_2O_2) layers. $\text{Bi}_{4-x}\text{La}_x\text{Ti}_3\text{O}_{12}$ (BLT) shows more promise for Nv-FeRAM than SBT because SBT films require high growth temperature and have small remnant polarization as compared to BLT [5,6]. In addition, BT and BLT have large electro-optical coefficient and hence are considered to be promising materials for integrated optics applications [4,7]. Further, their properties can be tailored for specific application by substitution at A- or B-sites, e.g., substitution of Bi-site with lanthanides ions, possessing comparable radius increases the electric polarization while the substitution of Ti-site with higher-valent cations tends to decrease the oxygen vacancy concentration in order to maintain the

electroneutrality [8–13]. This results in the improvement of polarization as well as lowering of the leakage current and the coercive field. While a number of studies have been devoted to see the effect of A- and B-site dopant on the electrical properties but very little has been reported on the optical properties [9–13]. In the present work, we have tried to investigate the effect of Mn doping on dielectric functions and optical band gap energy in BLT thin films using spectroscopic ellipsometry (SE). It is a nondestructive and powerful technique to investigate the optical response of materials, to measure simultaneously the thickness and dielectric function of a multilayer system. The two experimental quantities which are directly obtained through this technique are ψ and Δ . These parameters are indication of relative changes in the amplitude and the phase of a linearly polarized monochromatic incident light upon an oblique reflection from a sample surface. These are related to the optical and structural properties of the samples and defined by [14,15]

$$\rho = \frac{R_p}{R_s} = \tan \psi \cdot \exp(i\Delta) \quad (1)$$

where R_p and R_s are the complex reflection coefficients of the light polarized parallel and perpendicular to the plane of incidence respectively.

We analyzed the experimental data using a model (ambient/rough layer/BLTMn/Pt), wherein the Pt layer was thick enough so

* Corresponding author at: Department of Physics and Astrophysics, University of Delhi (DU), Delhi 110007, India. Tel.: +91 9871810585; fax: +91 011 2766796.

E-mail addresses: pgautam.phy.du@gmail.com (P. Gautam), ram_tandon@hotmail.com (R.P. Tandon).

that light could not propagate through it. A double Tauc–Lorentz (DTL) model [14,15] resulted in the best fit of the data. In order to judge the quality of the fit between the measured and fitted data using DTL model, the root-mean-square fractional error (MSE) σ is used, which is defined by [16]

$$\sigma^2 = \frac{1}{2J-K} \sum_{i=1}^J \left[\left(\frac{\psi_i^{\text{mod}} - \psi_i^{\text{exp}}}{\sigma_{\psi,i}^{\text{exp}}} \right)^2 + \left(\frac{\Delta_i^{\text{mod}} - \Delta_i^{\text{exp}}}{\sigma_{\Delta,i}^{\text{exp}}} \right)^2 \right]$$

$$= \frac{1}{2J-K} \chi^2 \quad (2)$$

where $\sigma_{\psi,\Delta}^{\text{exp}}$ are the measurement error bars. The pre-factor normalizes the function so MSE is not directly affected by change in the number of wavelengths (J is the number of ψ , Δ pairs) or number of ‘fit’ parameters (J) and K is the number of unknown model parameters.

2. Experimental procedure

The thin films of $\text{Bi}_{3.25}\text{La}_{0.75}\text{Ti}_{3-x}\text{Mn}_x\text{O}_{12}$ ($x = 0, 0.025, 0.05, 0.1$ and 0.2) with titular representation as BLTM-0, BLTM-1, BLTM-2, BLTM-3 and BLTM-4 respectively were deposited on Pt/Ti/SiO₂/Si (100) substrates by spin coating technique and is discussed in detail elsewhere [17]. Briefly, the precursor materials used to prepare the deposition solution were lanthanum acetate hydrate $[(\text{CH}_3\text{CO}_2)_3\text{La} \cdot x\text{H}_2\text{O}]$, bismuth acetate oxide $[\text{BiOCH}_2\text{COO}]$, titanium isopropoxide $[\text{Ti}(\text{OCH}(\text{CH}_3)_2)_4]$ and manganese acetate hydrate $[(\text{CH}_3\text{CO}_2)_2\text{Mn} \cdot 4\text{H}_2\text{O}]$. Glacial acetic acid and 2-methoxyethanol were selected as solvents. Part of the solvent was removed by distillation to obtain the desired concentrations. Water and ethylene glycol were used as chemical additives to modify the hydrolysis, condensation rate and to influence the drying characteristics of the sol–gel method. For the preparation of complex alkoxide solutions, Ti precursor solution was added with excess glacial acetic acids to the La, Bi and Mn acetate solids at room temperature with constant stirring for half an hour. The films were then deposited by spin-coating the solutions on Pt/Ti/SiO₂/Si (100) substrates at 2500 rpm for 20 s, drying at 240 °C for 3 min, and pre-firing at 350 °C for 10 min in air. This process was repeated several times to obtain the films of desired thickness and finally the films were annealed at 750 °C for 30 min in oxygen atmosphere. Atomic force microscope was used to study the morphology and roughness of thin films. Room temperature Raman spectra were recorded using inVia Renishaw Raman system, using a 514.5 nm argon ion excitation source. The ellipsometric measurements were done at room temperature, under incident angles of (65°, 70° and 75°) in wavelength range of 200–1700 nm (i.e., 0.72–6.2 eV) by using UV-near-IR V-VASE (J.A. Woollam, Inc.). The data fitting was done by using DTL model.

3. Results and discussion

Phase formation and surface morphology studies are discussed in detail in our earlier publication [17]. Structure and phase formation was studied using X-ray diffraction. These films are well crystalline and single phase with a bismuth-layered structure [17]. The symmetry of the structure was found to be orthorhombic with space group as *Pba*2. Fig. 1 shows the representative AFM image of BLTM-0. From AFM image analysis we found that these films were crack free and smooth with roughness in the range 5–10 nm. This range matches well with the roughness obtained from ellipsometry data fitting shown in Table 1.

It was observed from SEM and AFM study that with Mn-doping, the randomly (non *c*-axis) oriented grain increase while the plate like grains i.e. *c*-axis oriented grains decreases [17]. This affects the surface roughness of thin films. This observation was further supported from ellipsometry measurements that roughness was found to increase with the decrease in fraction of *c*-axis oriented grains.

Room temperatures Raman spectra of BLTM thin films are shown in Fig. 2(a) whereas Raman shift is shown in Fig. 2(b). From Raman spectra of BLTM thin films (in the studied composition range), not much modification in spectra is seen except some minor changes due to Mn doping. This clearly indicates that the BT structure is well preserved in the BLTM system. Also, Raman spectra of BLT and Mn modified BLT films are in well agreement

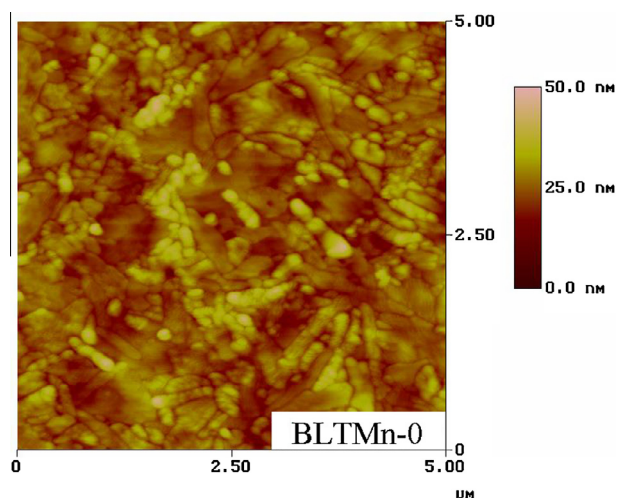


Fig. 1. Representative AFM image of BLTM-0.

with earlier reports [16,17]. The lower frequency modes at around 89 and 120 cm^{-1} (see in Fig. 2) are assigned as ‘rigid-layer’ modes (as these modes are related to the rigid movement of the Bi_2O_2 layer against the perovskite layer and from Bi^{3+} vibration in A-sites) [17–20].

The mode at around 265 cm^{-1} corresponds to the O–Ti–O bending vibration only. The modes $\sim 340 \text{ cm}^{-1}$ and 540 cm^{-1} modes are attributed to a combination of stretching and bending of TiO_6 octahedra, while the mode around 850 cm^{-1} is a pure stretching mode of TiO_6 . Since the pure stretching mode is unchanged with La substitution, the 540 cm^{-1} mode largely reflects the change in O–Ti–O bending vibration. Ti–O hybridization inside the TiO_6 is essential to ferroelectricity and can cause a structural distortion of TiO_6 due to the Ti displacement towards one of the six oxygen atoms [21]. The almost constant modes at 87 and 120 cm^{-1} , suggest that the B-site Mn^{3+} substitution has not affected the Bi^{3+} in A-sites and $(\text{Bi}_2\text{O}_2)^{2+}$ of this BLT system. However, for the TiO_6 octahedra (internal mode at about 850 cm^{-1}) [17,22,23], the B-sites Mn^{3+} substitution results in its lower frequency shift significantly. It is interesting to note that the Raman mode at about 706 cm^{-1} is associated with Ti–O symmetric stretch and this peak increases with increase with Mn-doping. The frequency of the new Raman mode is in accordance with that of the high-frequency phonon band of the octahedron with A_{1g} symmetry [24]. Therefore, it is reasonable to speculate that the new Raman mode resulting from the Mn–O vibrational mode is due to the substitution of Ti by Mn in the TiO_6 octahedron. The gradual enhancement of the new Raman mode with the increase in Mn-doping content further confirms the Mn substitution at the B site in BLTM thin film. All these results indicate that the heavier Mn^{3+} enters into the lattice by replacing the lighter Ti^{4+} at B-site.

From the Ellipsometric spectroscopy analysis of BLT and Mn-modified BLT thin films, the pseudo-dielectric functions $\langle \epsilon_1 \rangle$, $\langle \epsilon_2 \rangle$ for doped and pristine BLT thin films at the incident angle of 70° are shown in Fig. 3(a) and (b). The data obtained for ψ and Δ were best fitted with lowest MSE (σ) using a double Tauc Lorentz model. Further to be noted here, model and conclusions remain the same for the other angles of incidence (like 65° and 70°). The plots of evaluated real and imaginary dielectric functions (ϵ_1, ϵ_2) for the films with different Mn content are shown in Fig. 4. The values of pseudo-dielectric function obtained after fitting through DTL model are summarized in Table 1. The evaluated dielectric functions (Fig. 4) were consistent with Kramers–Kronig (K–K) relation [14,16]. K–K consistency of the real and imaginary dielectric functions provides a basis for ‘reasonable’ shape that the final

Download English Version:

<https://daneshyari.com/en/article/8000874>

Download Persian Version:

<https://daneshyari.com/article/8000874>

[Daneshyari.com](https://daneshyari.com)